RSC Advances

RSC Advances

www.rsc.org/advances

ROYAL SOCIETY OF CHEMISTRY

www.rsc.org/advances

ARTICLE TYPE

A facile design, highly efficient green synthetic strategy of peony flower-like SO$_4^{2-}$SnO$_2$-fly ash nano catalyst for the three component synthesis of serendipity product with dimedone in water

Kannan Thirumurthy and Ganesamoorthy Thirunarayanan*

5

We have first time successfully found serendipity product of 2-((2-((9-ethyl-9*H*-carbazol-3-yl)amino)-4,4-dimethyl-6-oxocyclohex-1-en-1-yl)(phenyl)methyl)-5,5-dimethylcyclohexane-1,3-dione derivatives
10 by utilized SO$_4^{2-}$SnO$_2$-fly ash nano catalyst in water. We have designed SO$_4^{2-}$SnO$_2$-fly ash nano catalyst it has good catalytic activity, easily separable, good reusability and notable industrial applications. The catalytic role of Sn-O has more affinity with carbonyl group of dimedone. The major component of fly ash (SiO$_2$) which may enhance the catalytic activity of oxidation processes. Within this incentive conversion of product could be rapid and high yielded. A facile designed, SO$_4^{2-}$SnO$_2$-fly ash nano catalyst
15 was characterized by Fourier transform infrared spectroscopy (FT-IR), confocal Raman spectroscopy, powder X-ray diffraction (PXRD), Field emission electron microscopy (FE-SEM), Energy dispersive X-ray spectroscopy (EDS and elemental color mapping), High resolution transmission electron microscopy (HR-TEM) and UV-Visible diffuse reflectance spectroscopy (UV-Vis DRS) techniques. The nano cube and peony flower like morphologies were found in FE-SEM and HR-TEM images. The flower
20 like SO$_4^{2-}$SnO$_2$-fly ash catalyst has highly stable nature was favorable for organic reaction. The crystalline nature, surface morphology, chemical composition and morphology of the reused SO$_4^{2-}$SnO$_2$-fly ash nano catalyst were proved by PXRD, FE-SEM, EDAX and HR-TEM analysis respectively. The facile designed SO$_4^{2-}$SnO$_2$-fly ash nano catalyst was versatile to both environmental and economical point of view. The synthesized serendipity product derivatives and byproducts were characterized by FT-IR, Nuclear
25 magnetic resonance (NMR) and High resolution-mass spectrometry (HR-MS).

Introduction

Modern organic chemists enthuse on environmental and economical abundant source of water, practically reliable for organic synthesis. It leads to organic synthesis in green manner
30 significantly. [1, 2] Recent decades, researchers paid much more interest on green synthetic approach with nano green catalyst for organic reactions. [3-5] By having this mind, we have taken account the environment pollutant and thermal power plant waste residue of fly ash to assist as a catalyst for organic reaction. Our group
35 earlier reported SO$_4^{2-}$-fly ash catalyst for Crossed-Aldol condensation. [6] This catalyst are not shown good catalytic activity in the present investigation. The demand for the suitable catalyst, we have concentrated on SnO$_2$ based catalyst. Since low toxic, thermally stable, less moisture native, high selectivity, good
40 catalytic activity, easily separable and reusable catalyst were found in recent articles. [7-11] The SnO$_2$ catalyst was utilized for numerous organic synthesis such as 2,4-diphenyl-4,6,7,8-tetrahydrochromen-5-one, [12] 4-Hydroxycoumarin *o*-alkylation, [13] 3,4-dihydropyrimidin-2(1*H*)-ones, [14] ketoesters, [15] esterification,

45 [16, 17] esterification of free fatty acids, [18] 1*H*-imidazole [19] and Mukaiyama aldol condensation. [20]
Carbazole based derivatives are virtuous medicinal application in breast cancer metastases, brain tumour, [21] and HIV. [22] Carbazole moiety possesses another vast attention in organic electronics
50 such as organic solar cells, organic light-emitting diodes (OLEDs), [23, 24] organic thin film transistors (OTFTs), [25] and organic semiconductors. [26] In this context our present investigation is to study the three component reaction with dimedone. In organic synthesis, dimedone is the key intermediate
55 for the synthesis of various products. In general, the three component reaction of dimedone, aniline and aldehydes gave the possible products and are reported such as 1,8-dioxodecahydroacridines, [27-32] acridine [33] and *N*-acridines. [34] Our present investigation deals the reaction with
60 3-amino-9-ethylcarbazole, dimedone and aldehyde in the presence of SO$_4^{2-}$SnO$_2$-fly ash catalyst. The products of this reaction, as (**6, 7** and **8**) were not furnished. Since, the products are unexpected of (**4 and 5**) and these are furnished shown in

Scheme. 1. Based on the earlier literature report, it states that the electron withdrawing nature of *m*-substituent amine (3-amino-9-ethylcarbazole) steric hindrance of electron density which may deferment the reaction. [35] Within this possibility products of (**6, 7** and **8**) was not furnished. The reaction was performed in the presence of aniline (**9**) under optimized condition the corresponding product of 2,2-dimethyl-9-phenyl-2,3,9,10-tetrahydroacridin-4(1H)-one (**10**) was furnished. Since, the authors believed that the reaction involves the above domino sequence of Knoevenagel condensation and Michael addition reactions.

To the best of our knowledge, first time, we have found serendipity product of 2-((2-((9-ethyl-9*H*-carbazol-3-yl)amino)-4,4-dimethyl-6-oxocyclohex-1-en-1-yl)(phenyl)methyl)-5,5-dimethylcyclohexane-1,3-dione derivatives in water. The heterogeneous catalyst $SO_4^{2-}SnO_2$-fly ash nano catalyst has been numerous advantages such as easily separable, economically reliable, eco-friendly and notable industrial applications.
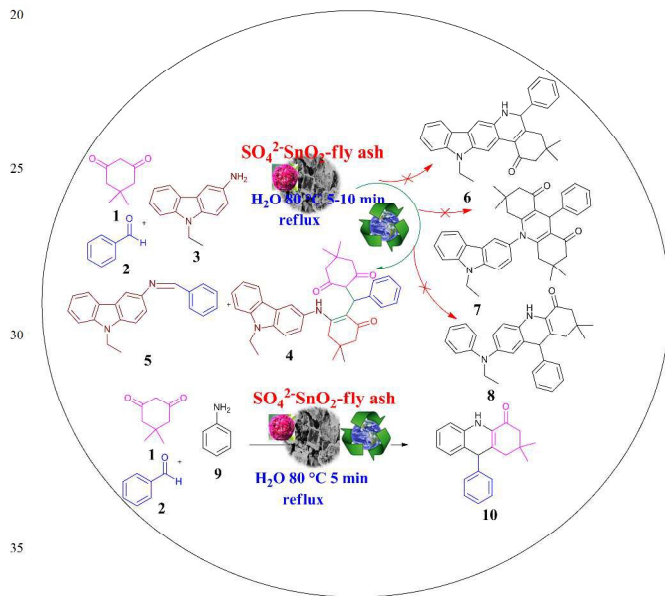
Scheme. 1 Screening of the $SO_4^{2-}SnO_2$-fly ash nano catalyst for serendipity product.

Results and discussion

Fourier transform infrared spectroscopy (FT-IR)

The FT-IR spectra of the facile designed SnO_2-fly ash, $SO_4^{2-}SnO_2$-fly ash catalysts are depicted in Fig. 1a-b. The absorption band was appeared at 968 cm^{-1} is assigned to the Si-O-Si band. The intense peak was appeared at 443 cm^{-1} which indicates Sn-O stretching vibration. The broad vibration peak observed at 643 cm^{-1} is referred that Sn-O-Sn symmetric and asymmetric frequency band are close agreement with earlier literature. [36] In addition to that the broad peak also appeared at 1124 cm^{-1} is assigned to asymmetric stretching vibration of SO_4^{2-} good agreement with earlier reports. [37, 38]
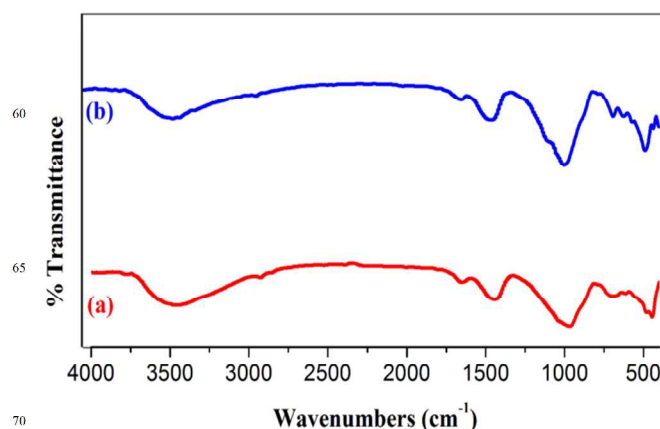
Fig. 1 FT-IR spectra of (a) SnO_2-fly ash, (b) $SO_4^{2-}SnO_2$-fly ash.

Confocal Raman spectroscopy

Fig. 2a-b depicts the confocal Raman spectra of SnO_2-fly ash and $SO_4^{2-}SnO_2$-fly ash respectively. Fig. 2a illustrates that the SiO_2 stretching vibration was observed at 859 cm^{-1} is close assessment of earlier reported value. [39] Fig. 2b reveals that the SiO_2 stretching band was shifted to the higher region, which is specified at 1122 cm^{-1}. The broad high intensity of peak observed at 794 cm^{-1} is assigned as SO_4^{2-} bending vibration which is good agreement with earlier reported Raman shift. [40] From the Fig 2a and 2b spectra results, SnO_2 Raman shifts were found at 614, 816, 1270 and 2211 cm^{-1} which are represents the Sn-O-Sn stretching mode coincide in earlier literature. [41, 42]
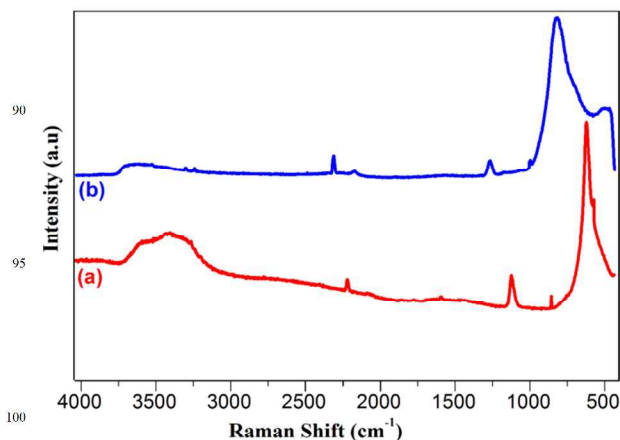
Fig. 2 Confocal Raman spectra of (a) SnO_2-fly ash, (b) $SO_4^{2-}SnO_2$-fly ash.

Powder X-ray diffraction (PXRD)

The crystalline phase of SnO_2-fly ash and $SO_4^{2-}SnO_2$-fly ash catalysts were analysed by powder XRD patterns and illustrated in Fig. 3a-b. The diffraction patterns of catalysts were indexed by mullite, quartz and magnetite [43, 44] (Fig. 3a-b). A diffraction pattern appeared at 37.10 2θ (°) reveals the presence of SnO_2. The corresponding 2θ (°) value of d spacing value is 1.11 Å and plane

is [3 3 1] which is good agreement with earlier literature of SnO_2 (JCPDS card No. 50-1429 space group Pa3 and a_0=4.870 Å). [45] The new diffraction peaks was observed at 64.98 2θ (°) which may represent the SO_4^{2-} [46] In addition to that the diffraction patterns were also observed at 14.10 and 29.28 2θ (°) (indicated by cube). The corresponding planes are [1 1 1] and [2 2 2] agreed the d spacing value as 2.81 and 1.40 Å respectively. As a result crystalline phase of SnO_2 which were good agreement with earlier literature value of SnO_2 (JCPDS card No. 50-1429).
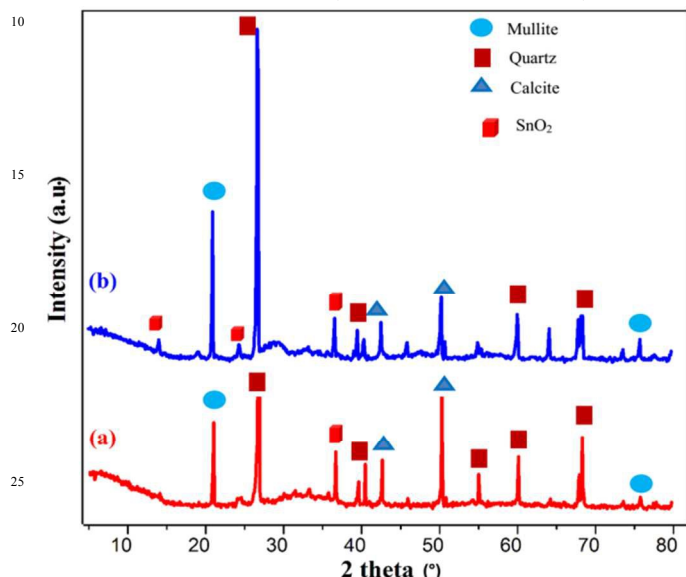
Fig. 3 PXRD-patterns of (a) SnO_2-fly ash (b) $SO_4^{2-}SnO_2$-fly ash.

Field emission scanning electron microscopy (FE-SEM)

The nano structure and surface morphology of the SnO_2-fly ash and $SO_4^{2-}SnO_2$-fly ash catalysts were analyzed by FE-SEM and depict in Fig. 4a-d.
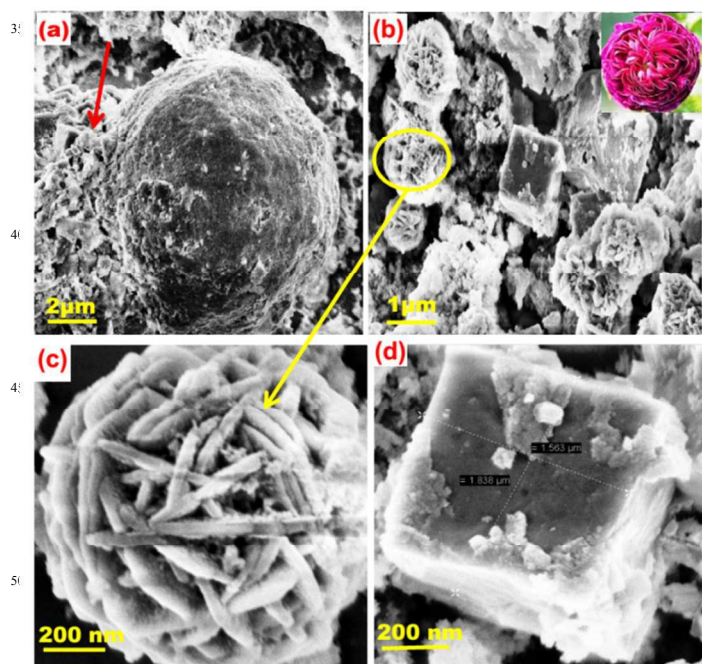

Fig. 4 FE-SEM images of (a) SnO_2-fly ash (b-d) $SO_4^{2-}SnO_2$-fly ash, scale bars (a) 2 μm, (b) 1 μm (c, d) 200 nm.

Fig. 4a image reveals that the SnO_2-fly ash, the cubic structures which are coexists on globular shape with size of 2 μm. Fig. 4b-d described the surface morphology of the facile designed $SO_4^{2-}SnO_2$-fly ash catalyst. Fig. 4b shows the fine shape nanostructure of cubic and numerous of peony like (peony flower inserted) nano flower (indicated yellow spherical) was seemed, about 1 μm. The close up view of the nano cubic and nano flower individual surface morphology of 200 nm which as shown in Fig. 4c, 4d. Fig. 4c seen the flower like regular arrangement was attained and flower petals are uniform dispersal, within the constructed space. Fig. 4d image seems that the fine shape and smooth face of nano cube was clearly observed. In this observation concise, designed catalyst is regularly arranged within the particles.

Field emission scanning electron microscopy elemental color mapping

The chemical composition, of $SO_4^{2-}SnO_2$-fly ash was examined by FE-SEM elemental color mapping. The result provides the uniform distribution of chemical composition, as illustrated in Fig. 5. The individual elemental color mapping (S, Sn, Si, Al, O, Ca, Fe and Mg) is displayed in Fig. 5b-5i. The fly ash comprises elements (Al, O, Si, Ca, Fe and Mg) ensuing, Sn and S elements are present in facile modified catalyst. Noteworthy no other element appeared, this result further noticed $SO_4^{2-}SnO_2$-fly ash catalyst is in pure form.
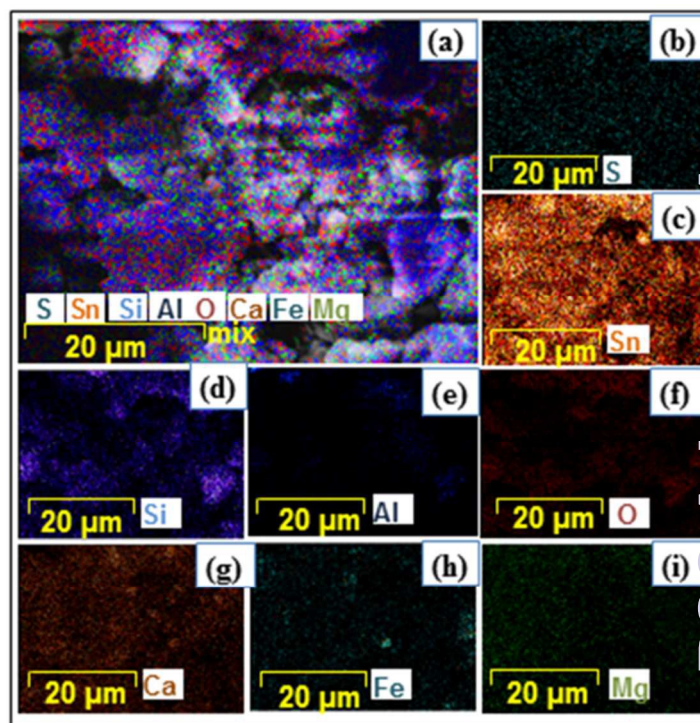
**Fig. 5** FE-SEM elemental color mapping of (a) $SO_4^{2-}SnO_2$-fly ash mix, (b) S, (c) Sn, (d) Si, (e) Al, (f) O, (g) Ca, (h) Fe, and (i) Mg, scale bars (a-i) 20 μm.

Energy dispersive X-ray analysis (EDS)

The chemical composition of SnO_2-fly ash and $SO_4^{2-}SnO_2$-fly ash was examined by EDS analysis. The facile designed SnO_2-fly ash components of Si, Mg, Ca, Al, Fe, O and Sn shown in Fig. 6a.

Fig. 6b shows that the facile designed SO_4^{2-}-SnO_2-fly ash peony like nano flower and nano cube catalyst chemical composition are similar to Fig 6a, however in addition to that S element also appeared. The catalyst elemental composition, weight and atomic
5 weight percentage is given in ESI Table S1.
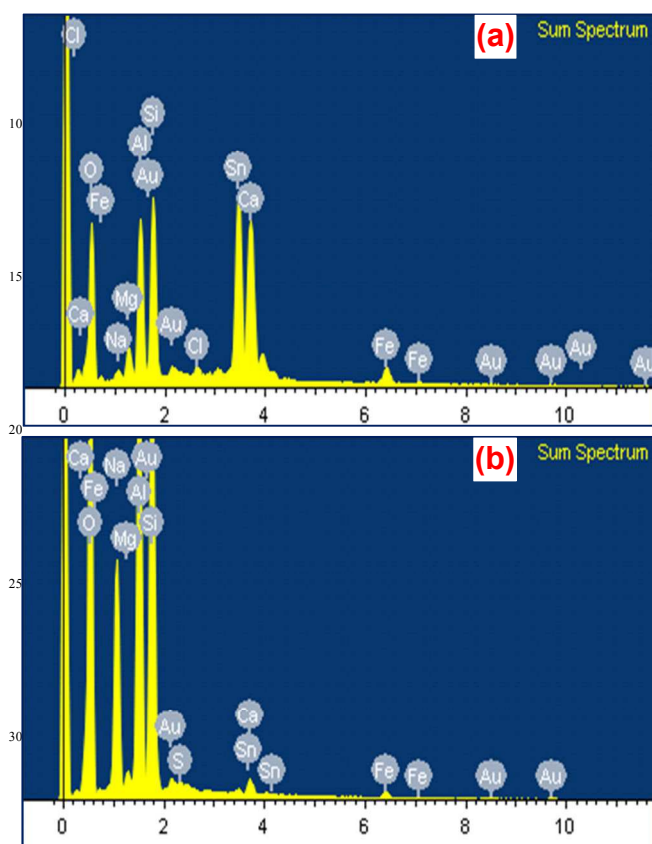
Fig. 6 EDS spectra of (a) SnO_2-fly ash (b) SO_4^{2-}-SnO_2-fly ash

High resolution transmission electron microscopy (HR-TEM)

The nano cube and peony like nano flower morphology of
40 SO_4^{2-}-SnO_2-fly ash was examined by High resolution transmission electron microscopy (HR-TEM) shown in Fig.7a-7f. Fig. 7a reveals that the flawless nano cube was observed, it seen smooth edges of cube length, width and height. The nano cube parameters were displayed, nano cube length is 520 nm, width is
45 89 nm and height is 459 nm respectively. The peony flower like nano flower morphology observed of 0.2 μm. The Fast Fourier Transform (FFT) (inserted) it seemed, flower like uniform spots shown in Fig. 7b. The nano flower in order to further assessed, it seen nano flower petals about 50 nm (nano petals FFT inserted)
50 shown in Fig. 7c. The nano flower morphology have modest characters such as strongly bonded with atoms, highly stable nature, high exposure of active facets, high degree of dispersion and highly crystalline nature. [47] The HR-TEM lattice fringes was measured of 0.21 nm, 0.27 nm (FFT inserted) depicts in Fig. 7d.
55 Fig. 7e depicts the growth direction of cube orientation planes [1 1 1], [2 2 2] and [3 3 1] are displayed in SAED pattern (FFT inserted). Fig. 7f close reviewed SAED pattern it seems cube like regular diffraction pattern. From the results suggest that facile designed SO_4^{2-}-SnO_2-fly ash catalyst has good crystalline phase.
60
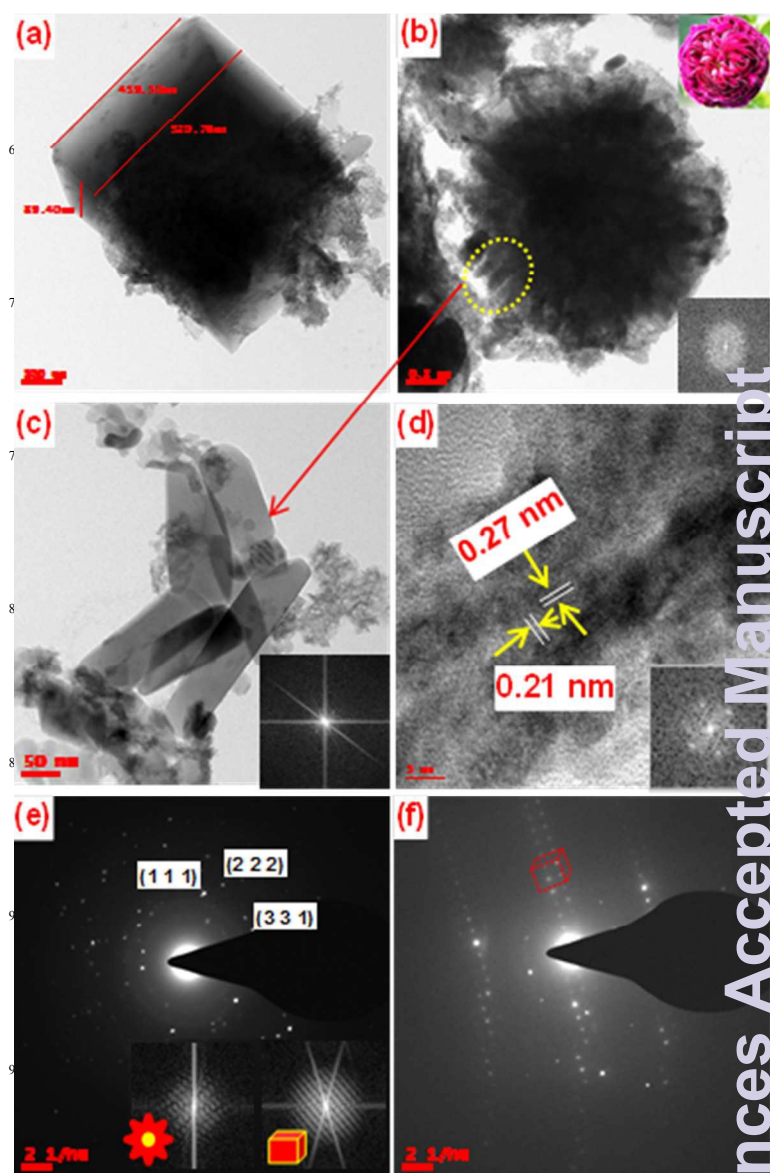
100 **Fig. 7** HR-TEM images of SO_4^{2-}-SnO_2-fly ash (a) nano cube, (b) nano flower, (c) nano petal, (scale bars (a) 100 nm, (b) 0.2 μm, (c) 50 nm), (d) HR-TEM 5 nm, (e, f) SAED patterns 2 1/nm.

Optimization of the reaction conditions

105 To find the noticeable reaction condition for unusual product of 2-((2-((9-ethyl-9*H*-carbazol-3-yl)amino)-4,4-dimethyl-6-oxocyclohex-1-en-1-yl)(phenyl)methyl)-5,5-dimethylcyclohexane-1,3-dione **4a** and by product (*E*)-*N*-benzylidene-9-ethyl-9*H*-carbazol-3-amine **5a** in water. The
110 reaction mixture of dimedone (1 mmol 152 mg), benzaldehyde (1 mmol 0.1 mL) and 3-amino-9-ethylcarbazole (1 mmol 210 mg) in the absence of catalyst in water at 95 °C for 8 h. The resulting in the absence of catalyst no product was furnished Table 1 entry 1. Then we have attempted the reaction in the presence of fly ash
115 catalyst at 95 °C for 5 h. The resulting trace amount of yield of **4a** and 12% **5a** yield was furnished shown in Table 1 entry 2. The next examination of the reaction in the presence of SO_4^{2-}-fly ash

catalyst at 85 °C for 3.5 h. This reaction condition, only trace amount of **4a** and 17% **5a** was isolated shown in Table 1 entry 3.

Table 1 Optimization of the reaction conditions^a
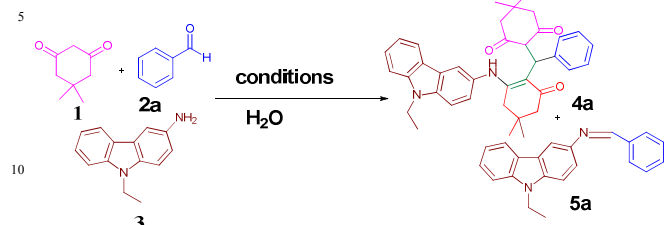
| Entry	Catalyst^b	Time (h)	Temperature (°C)	Yield^c (%)	
				4a	5a
1	No catalyst	8	95	No reaction	
2	Fly ash	5	95	trace	12
3	SO_4^{2-}-fly ash	3.5	85	trace	17
4	H_2SO_4	8	85	trace	10
5	CuO	10	85	---	26
6	Bi_2O_3	7	95	7	33
7	ZrO	12	95	---	18
8	MgO	12	95	---	10
9	SnO_2	2.5	95	10	40
10	CuO-fly ash	12	95	---	38
11	Bi_2O_3-fly ash	3	85	13	47
12	ZrO-fly ash	8	85	---	28
13	SnO_2-fly ash	1	80	18	63
14	$SO_4^{2-}Bi_2O_3$-fly ash	1	80	20	26
15	$SO_4^{2-}SnO_2$-fly ash 1 wt%	20 (min)	80	56	16
16	$SO_4^{2-}SnO_2$-fly ash 3 wt%	10 (min)	80	68	14
17	$SO_4^{2-}SnO_2$-fly ash 5 wt%	10 (min)	80	73	12

^{a}Reaction condition: dimedone, benzaldehyde and 3-amino-9-ethylcarbazole (1 mmol scale). ^{b}performed catalyst. ^{c}Isolated yield.

In this observation to find the catalytic efficiency of sulfuric acid in this reaction, however it did not promote the reaction. Next we screened the catalytic efficiency of five metal oxides (CuO, ZrO, MgO, Bi_2O_3 and SnO_2) of the present reaction. In these conditions **5a** only furnished Table 1 entry 5, 7 and 8. However these catalysts (CuO, ZrO, MgO) not supported for product **4a** and **5a.** The good selectivity of the Sn and Bi metals has high oxidation activity, which is addressed on earlier literature.[48] In this connection, presence of Bi_2O_3 and SnO_2 catalysts to afford trace amount of 4a. Next we have examined metal oxide loaded fly ash catalyst (CuO-fly ash and ZrO-fly ash) these catalysts furnished only **5a** yield depicted in Table 1 entry 10. In this continuous screening Table 1 entry 3, 4, 9, 11 and 13 the unusual product of **4a** compound was appeared. As results and well documented in the presence of fly ash, super acid condition with

SnO_2 catalyst support product **4a** furnished. In this mind we have focused on sulfated metal oxide fly ash catalyst for the present reaction. The reaction was performed with $SO_4^{2-}Bi_2O_3$-fly ash catalyst support the yield 20% compound **4a** was obtained and illustrated Table 1 entry 14. Our prime motto and aim was improve unusual product, in this intension we studied the different weight percentage of $SO_4^{2-}SnO_2$-fly ash (SnO_2 1, 3, 5 wt%) catalyst in the reaction. The yield of **4a** was successfully improved to 56% by using 1wt% of $SO_4^{2-}SnO_2$-fly ash. In this observation $SO_4^{2-}SnO_2$-fly ash catalyst (3, 5 wt%) and evaluated the reaction shown in Table 1 entry 16, 17.
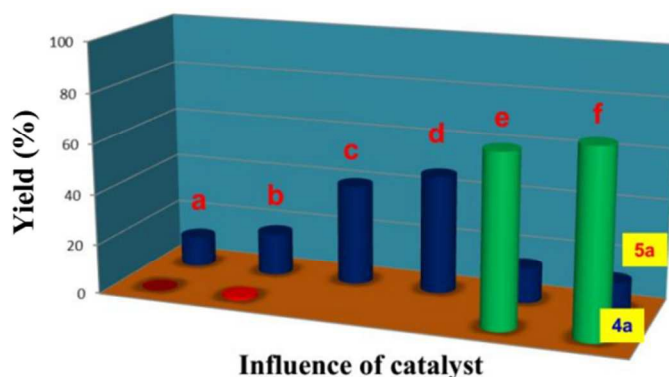
Fig. 8 Optimization of catalyst (a) fly ash, (b) SO_4^{2-}-fly ash, (c) metal oxides (CuO, Bi_2O_3, ZrO, MgO, and SnO_2), (d) metal oxides loaded fly ash (CuO, Bi_2O_3, ZrO, MgO, and SnO_2), (e, f) $SO_4^{2-}SnO_2$-fly ash (3, 5 wt%).

Inspired by the optimal reaction condition, we have designed further entries, of electron withdrawing and donating substitute groups of aromatic benzaldehyde shown in Table 2 (entry 1-8). The electron withdrawing group of benzaldehydes smoothly went the reaction, with good yield. The bulky group of 2-chloro-6-methoxy-3-quinolinecarboxaldehyde gave good yield within 10 min Table 2 entry 2. Specifically electron withdrawing group of 4-trifluoromethylbenzaldehyde, 4-methylthiobenzaldehyde and 2-thiophenecarboxaldehye to afford excellent yield of unusual product with short reaction time showed in Table 2 entry 3, 5 and 7. When the substrate contain electron donating group minimum time required to convert product.

Table 2 Synthesis of 2-((2-((9-ethyl-9H-carbaol-3-yl)amino)-4,4-dimethyl-6-oxocyclohex-1-en-1-yl)(phenyl)methyl)-5,5-dimethylcyclohexane-1,3-dione derivatives (**4a-4g**)

Entry	RCHO	Product[b]		Time (min)	Yield (%)[c]	
					4a-4g	**5a-5g**
1	benzaldehyde	**4a**	**5a**	10	73	12
2	methoxy-quinoline-carbaldehyde-Cl	**4b**	**5b**	10	79	10
3	F₃C-benzaldehyde	**4c**	**5c**	5	85	7
4	methoxy-benzaldehyde	**4d**	**5d**	5	70	14
5	H₃CS-benzaldehyde	**4e**	**5e**	7	87	9
6	NO₂-benzaldehyde	**4f**	**5f**	8	68	22
7	thiophene-carbaldehyde	**4g**	**5g**	5	85	10

[a]Reactions were carried out with dimedone, substituted benzaldehyde, 3-amino-9-ethylcarbazole (1 mmol scale), SO_4^{2-}-SnO_2-fly ash catalyst (50 mg) and water as solvent at 80 °C for 5-10 min. [b]Isolated product. [c]Isolated yield.

Reusability of SO_4^{2-}-SnO_2-fly ash nano green catalyst

To evaluate the reusability efficacy heterogeneous SO_4^{2-}-SnO_2-fly ash nano catalyst, in the formation of unusual 2-((2-((9-ethyl-9H-carbazol-3-yl)amino)-4,4-dimethyl-6-oxocyclohex-1-en-1-yl)(4-(trifluoromethyl)phenyl)methyl)-5,5-dimethylcyclohexane-1,3-dione under optimized condition. The reused solid SO_4^{2-}-SnO_2-fly ash nano catalyst was recovered from reaction mixture by employing filtration technique. The catalyst was purified with DCM (20 mL) and the catalyst was dried in hot air oven at 130 °C for 1 h. The similar processes were continued up to sixth consecutive run. The reusability potential of SO_4^{2-}-SnO_2-fly ash catalyst was examined by up to sixth reaction cycles. The conversion of yield was evaluated in the terms of turn-over number (TON_1, TON_2) and turn-over frequency (TOF_1, TOF_2) shown in Table 3. Recycling experiment of SO_4^{2-}-SnO_2-fly ash nano catalyst shown in Fig 9. The account concise of fresh catalyst and sixth cycles run catalyst did not lead to any significant decay in its catalytic activity. However the trivial time required to conversion of product.
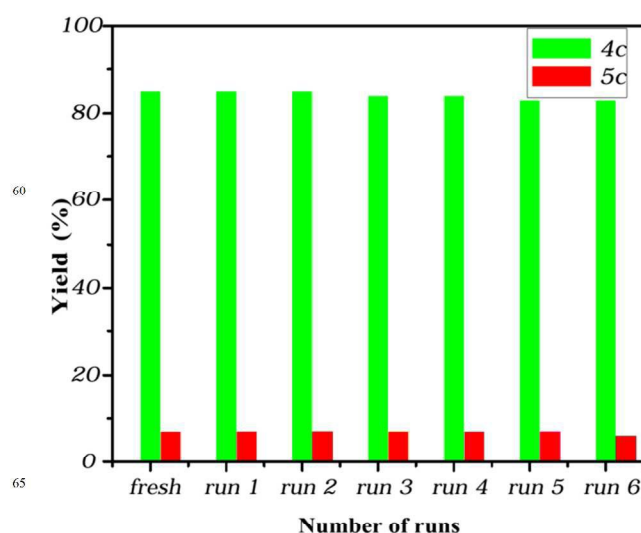
Fig. 9 Recycling experiment of SO_4^{2-}-SnO_2-fly ash nano catalyst

Table 3 Recycling potential of SO_4^{2-}-SnO_2-fly ash catalyst for **4c** and **5c**

Entry	No. of runs	Time (min)	Yield (%)	TON_1	TON_2	TOF_1	TOF_2
1	fresh	5	85:7	5.1	0.42	0.017	0.001
2	run 1	5	85:7	5.1	0.42	0.017	0.001
3	run 2	5	85:7	5.1	0.42	0.017	0.001
4	run 3	7	84:7	5.0	0.42	0.011	0.001
5	run 4	8	84:7	5.0	0.42	0.010	0.0008
6	run 5	8	83:7	4.9	0.42	0.010	0.0008
7	run 6	8	83:6	4.9	0.36	0.010	0.0007

Characterization techniques of reused SO_4^{2-}-SnO_2-fly ash catalyst

The catalyst crystalline nature and surface morphology of sixth reaction run SO_4^{2-}-SnO_2-fly ash nano catalyst was examined by Powder XRD, FE-SEM, EDS and HR-TEM techniques. Fig. 10a depicts sixth cycles run SO_4^{2-}-SnO_2-fly ash catalyst are shown similar to fresh catalyst diffraction pattern. The sixth consecutive run catalyst morphology was examined by FE-SEM technique. Fig. 10b-c FE-SEM reveal that the peony like nano flower and nano cube morphology respectively. The nano flower and nano cube regular arrangement of particle 200 nm which is similar to freshly catalyst morphology. From this morphology studies we concise, the reused SO_4^{2-}-SnO_2-fly ash catalyst no morphology changes even after sixth successive run. The EDS spectrum shown in Fig. 10d and the chemical composition weight percentage were given in ESI Table S1. The HR-TEM images deals that the sixth reaction run catalyst possess no noticeable change in nano flower (FFT images inset) shown in 10e. The smooth face of nano cubic morphology was displayed in Fig. 10f. From the results sixth reaction run catalyst not affected morphology. The SAED pattern diffraction spots seen regular arrangement shown in Fig.10h.
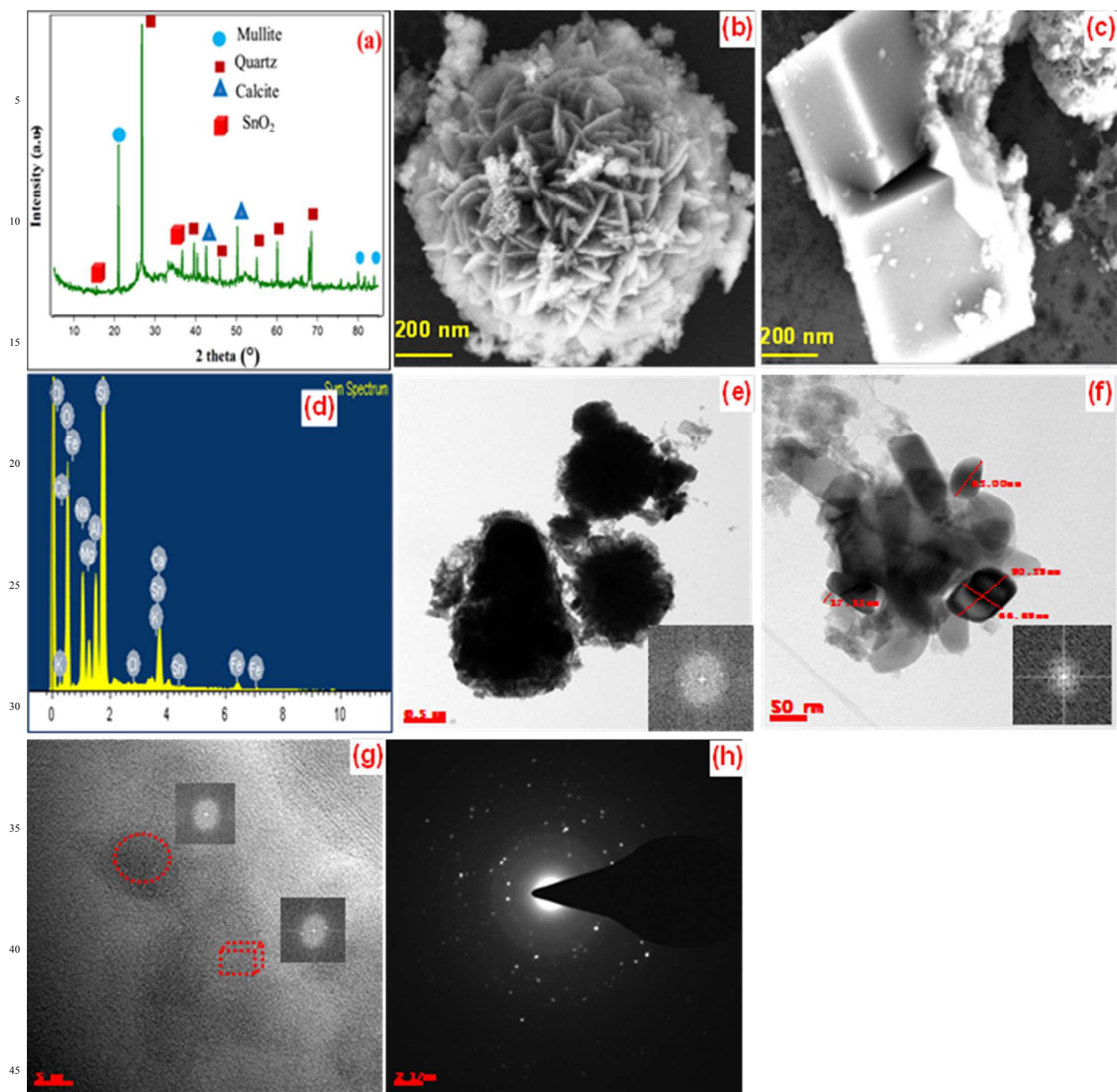
**Fig. 10** Sixth run SO_4^{2-}-SnO_2-fly ash catalyst (a) powder XRD (b, c) FE-SEM images (d) EDS (e-g) HR-TEM images (h) SAED patterns 2 1/nm.

Probing of SO_4^{2-}-SnO_2-fly ash for serendipity product

The significant scope of the fly ash (type C) major component of (SiO_2) to enhance, the catalytic activity for oxidation processes. [49] The catalytic role of SnO_2 to activate the electrophilic nature of carbonyl groups (dimedone and aldehyde). The main precious character, of Sn metal was eagerly coordinates with carbonyl group and readily form adduct. In this observation Sn metal has been good selectivity for oxidation processes. [50] In addition, the catalytic nature of SO_4^{2-} to improve the oxidation reaction. [51] Within this connection serendipity product could be rapid with high yield.

Plausible mechanism of serendipity product

The plausible mechanism pathway was described the formation of serendipity product of 2-((2-((9-ethyl-9*H*-carbazol-3-yl)amino)-4,4-dimethyl-6-oxocyclohex-1-en-1-yl)(phenyl)methyl)-5,5-dimethylcyclohexane-1,3-dione. The electronic configuration of Sn and Si empty d orbital promising to form bond with electronegative nature of dimedone.[52] The catalytic probe of Sn/SiO_2 would be assisted to improve the reactive species and product selectivity.[53, 54] In this favorable observation, we have designed SO_4^{2-}-SnO_2-fly ash nano catalyst supported this reaction under optimal condition, resulting the furnished product might be rapid and high yield. The following sequence of mechanism has outlined in Scheme **2**. The well documented, reaction pathway of dimedone with benzaldehyde to afford adduct **IV** through Knoevenagel condensation. In addition to that the SO_4^{2-}-SnO_2-fly ash eagerly coordinates with carbonyl group of dimedone and benzaldehyde enhanced the reaction activity.
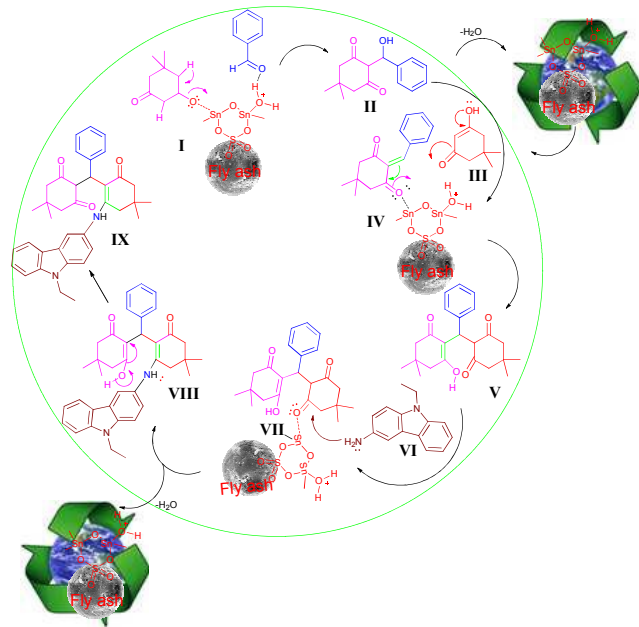
Scheme. 2 Plausible reaction mechanism of serendipity product

The next step nucleophilic Michael addition followed by enol formation was obtained, subsequent the catalyst was regenerated. Then catalyst again involved in the reaction and coordinates with dimedone and its furnished with the product **V**. The next step **VI** (3-amino-9-ethylcarbazole) react with compound **V**, which under

goes the 1,4-Michael addition and it afford compound **VII**. The subsequent reaction between unreacted benzaldehyde and **VI** it might lead to (*E*)-*N*-benzylidene-9-ethyl-9H-carbazol-3-amine. The final step is enol formation, followed by deprotonating to afford compound **IX** and catalyst was regenerated.

Conclusions

In summary, we have first time successfully found serendipity product of 2-((2-((9-ethyl-9*H*-carbazol-3-yl)amino)-4,4-dimethyl-6-oxocyclohex-1-en-1-yl)(phenyl)methyl)-5,5-dimethylcyclohexane-1,3-dione derivatives (**4a-4g**) in water. The environmental challenge reprocessing solid waste residue, fly ash was successfully designed SO_4^{2-}-SnO_2-fly ash as a heterogeneous green protocol to three component reaction. In addition, we have demonstrated the nano catalyst was attractive in view of its low cost, simple preparation method, easy to handle, reusable, easily separable from reaction mixture and notable industrial applications. After six consecutive run SO_4^{2-}-SnO_2-fly ash nano green catalyst provided good yield for unusual 2-((2-((9-ethyl-9*H*-carbazol-3-yl)amino)-4,4-dimethyl-6-oxocyclohex-1-en-1-yl)(4-(trifluoromethyl)phenyl)methyl)-5,5-dimethylcyclohexane-1,3-dione. The crystalline nature and surface morphology of six successive runs SO_4^{2-}-SnO_2-fly ash nano catalyst was examined by PXRD, FE-SEM, EDS and HR-TEM. From these studies we observed no appreciable changes in the catalytic nature.

Experimental

Materials and methods

All the chemicals were procured from Sigma Aldrich, Merck and SRL India. Fly ash material (type C) was collected from Thermal Power Plant-II, Neyveli Lignite Corporation (NLC), Neyveli, Tamil Nadu, India.

Fourier Transform Infrared spectra (KBr 4000-400 cm^{-1}) were recorded on an Avatar-300 Fourier transform spectrophotometer. Confocal Raman spectra of the samples were collected on Wi Tec Alpha 300. The crystalline phase of SnO_2-fly ash and SO_4^{2-}-SnO_2-fly ash catalyst, were characterized by Powder X-ray diffraction (PXRD) on D8 Advance Bruker diffractometer operating at 230 V, 50 Hz, 6.5 KVA with Cu Kα source (λ=1.5418 Å). The nano structure and surface morphology of SO_4^{2-}-SnO_2-fly ash were characterized by Field-emission scanning electron microscopy (FE-SEM) (55, Carl Zeiss). The elemental composition analyzed by Energy dispersive X-ray spectrometer (EDS) working at 200 kV. The samples were prepared by dispersion method on glass slide with gold coating. The nano cube and peony like nano flower SO_4^{2-}-SnO_2-fly ash catalyst were recorded, on High resolution transmission electron microscopy (HR-TEM) (Tecnai G2 operating at 120 kV). The samples were dispersed on carbon-coated TEM grid (200 mesh). The UV-visible diffuse reflectance spectra (UV-Vis DRS) of SnO_2-fly ash and SO_4^{2-}-SnO_2-fly ash were recorded on (Shimadzu UV-3600 UV-visible-NIR spectrometer). UV-Vis DRS samples was prepared by pellet assemble method, using $BaSO_4$ as reference. Melting points of synthesized compounds were determined in open glass capillaries on Mettler FP51 melting point apparatus and were uncorrected. The NMR spectra of unknown compounds were recorded in Bruker AVIII 5000 spectrometer operating, at 400 MHz for ^{1}H NMR spectra and 125 MHz for ^{13}C NMR spectra in $CDCl_3$ solvent using tetra methyl silane as internal standard. HR-MS (ESI) analyses were recorded on Bruker Maxis instrument (Maxis 10138).

Facile designed SO$_4^{2-}$SnO$_2$-fly ash nano catalyst.

In a typical procedure for SO$_4^{2-}$SnO$_2$-fly ash catalyst, SnCl$_4$.5H$_2$O (331 mg 5 wt%) was taken in clean beaker, it dissolved in 10 mL of conductivity water. This solution was added drop wise to the sulfated fly ash mixture and it was vigorously stirred for 10 min. Followed by the addition of aqueous ammonia solution (5 mL) was added into the mixture under constant stirring. The mixture was maintained at 80 ºC for 1 h. After 1 h stirring the mixture was transferred into a Teflon-lined stainless-steel autoclave, sealed and heated at 116 °C for 3 h. During the process, the pressure was maintained at 30 psi. Then it dried in an oven at 130 °C for 1 h. Then calcined at 500 ºC for 3 h in a muffle furnace to get final catalyst. The catalyst preparation method is shown in Fig. 11 as schematic representation.
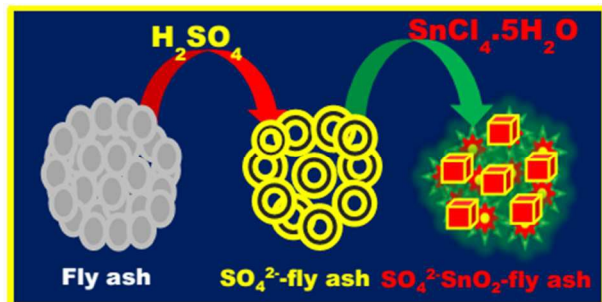
Fig. 11 preparation method of SO$_4^{2-}$SnO$_2$-fly ash nano catalyst

General procedure for synthesis of serendipity products

A clean 25 mL round-bottom flask was charged with the dimedone (1 mmol), substituted benzaldehyde (1 mmol), 3-amino-9-ethylcarbazole (1 mmol) and SO$_4^{2-}$SnO$_2$-fly ash catalyst (50 mg) in water (15 mL) was refluxed at 80 ºC for 5-10 minutes. The completion of the reaction was monitored by TLC (ethyl acetate and hexane as an eluent 20%). After completion of the reaction mixture was cooled to ambient temperature. Then dichloromethane (20 mL) was added to reaction mixture the organic and aqueous layers were separated. Insoluble solid SO$_4^{2-}$SnO$_2$-fly ash nano catalyst was washed with water and dichloromethane (20 mL) its dried in hot air oven at 130 ºC for 1 h. The dried SO$_4^{2-}$SnO$_2$-fly ash was reused for further reaction run up to sixth run. The organic layer filtered, dried on anhydrous Na$_2$SO$_4$ and organic solvent was removed using rotary evaporator. The crude product was purified by Column chromatography, through silica gel (200 mesh) with (20%) 80:20 hexane/ethyl acetate as eluent to the desired pure unusual products **4a-4g** and **5a-5g**. The purified compounds were confirmed, by physical constants and spectral techniques (FT-IR, NMR and HR-MS).

Characterization data for 2-((2-((9-ethyl-9H-carbazol-3-yl)amino)-4,4-dimethyl-6-oxocyclohex-1-en-1-yl)(phenyl)methyl)-5,5-dimethylcyclohexane-1,3-dione derivatives (4a-4g) and (E)-N-benzylidene-9-ethyl-9H-carbazol-3-amine derivatives (5a-5g) (Table 2 entry 1-7)

2-((2-((9-ethyl-9H-carbazol-3-yl)amino)-4,4-dimethyl-6-oxocyclohex-1-en-1-yl)(phenyl)methyl)-5,5-dimethylcyclohexane-1,3-dione (Table 2, entry 1, 4a)

Isolated as a yellow solid Yield (414 mg 73%); m.p. 82-83 °C; FT-IR 3046, 2931, 1594 cm^{-1}; ^{1}H NMR (400 MHz, CDCl$_3$, δ$_H$; 8.02 (s, 1H, NH), 7.51 (d, J=8.0 Hz, 1H, ArH), 7.44-7.42 (m, 3H, ArH), 7.36 (d, J=8.0 Hz, 2H, ArH), 7.30 (s, 3H, ArH), 7.23 (d, J=8.5 Hz , 1H, ArH), 7.18 (t, J=7.0, 1H, ArH), 7.17 -7.13 (m, 1H, ArH), 6.94-6.91 (dd, J$_1$=4.0 Hz, J$_2$=4.0 Hz, 1H, ArH), 5.59 (s, 1H, CH), 4.33 (q, J=7.2 Hz, 2H, CH$_2$), 2.51 (d, J=4.0 Hz, 1H, CH$_2$), 2.43 (d, J=4.0 Hz, 3H, CH$_2$), 2.32 (t, J=8.0 Hz, 2H, CH$_2$), 2.36 (s, 1H, CH$_2$), 2.18 (s, 1H, CH$_2$), 1.45 (t, J=8.0 Hz, 3H, CH$_3$), 1.27 (d, J=12.0 Hz, 5H, CH$_3$), 1.17 (d, J=8.0 Hz, 2H, CH$_3$), 1.12 (s, 3H, CH$_3$), 0.99 (s, 1H, CH$_3$), 0.92 (s, 1H, CH$_3$); ^{13}C NMR (125 MHz, CDCl$_3$) δ$_C$: 190.54, 189.43, 158.09, 140.43, 138.91, 138.14, 134.57, 128.26, 128.10, 126.93, 126.83, 126.35, 125.88, 125.46, 125.39, 123.69, 122.49, 122.43, 120.43, 118.03, 115.62, 109.02, 108.38, 106.41, 50.33, 49.78, 47.10, 46.49, 37.53, 32.80, 31.44, 29.75, 29.68, 28.63, 28.20, 27.43, 13.86; HRMS (ESI/[M + H]$^+$) calcd for C$_{37}$H$_{40}$N$_2$O$_3$; 561.3109, found 561.3117.

2-((2-chloro-3,4-dihydroquinolin-3-yl)(2-((9-ethyl-9H-carbazol-3-yl)amino)-4,4-dimethyl-6-oxocyclohex-1-en-1-yl)methyl)-5,5-dimethylcyclohexane-1,3-dione (Table 2, entry 2, 4b)

Isolated as a brown solid Yield (554 mg 79%); m.p. 112-113 °C; FT-IR 3046, 2931, 1621, 536 cm^{-1}; ^{1}H NMR (400 MHz, CDCl$_3$) δ$_H$; 9.07 (s, 1H, NH), 8.87 (s, 1H, ArH), 8.10 (t, J=4.0 Hz, 1H, ArH), 7.88 (d, J=8 Hz, 1H, ArH), 7.54 (d, J=4.0 Hz, 1H, ArH), 7.47 (t, J=8.0 Hz, 2H, ArH), 7.39-7.35 (m, 3H, ArH), 7.24 (s, 2H, ArH), 7.08 (s, 1H, ArH), 5.26 (s, 1H, CH), 4.31 (q, J=7.0 Hz, 2H, CH$_2$), 3.87 (s, 3H, OCH$_3$), 2.57 (d, J=8.0 Hz, 2H, CH$_2$), 2.44 (d, J=8.0 Hz, 2H, CH$_2$), 2.33 (d, J=12.0 Hz, 2H, CH$_2$), 2.19 (d, J=8.0, 2H, CH$_2$), 1.41 (t, J=4.0 Hz, 3H, CH$_3$), 1.22 (s, 3H, CH$_3$), 1.17 (s, 3H, CH$_3$), 1.11 (d, J=8.0 Hz, 4H, CH$_3$), 1.04 (s, 1H, CH$_3$), 0.93 (s, 1H, CH$_3$); ^{13}C NMR (125 MHz, CDCl$_3$) δ$_C$; 200.11, 196.42, 158.30, 152.47, 147.72, 144.29, 142.83, 140.53, 139.31, 136.52, 135.67, 129.56, 129.22, 128.33, 127.97, 126.46, 126.12, 124.41, 123.51, 123.34, 122.99, 122.38, 120.65, 120.07, 119.14, 118.22, 113.44, 108.92, 108.81, 105.77, 55.63, 53.54, 50.14, 44.92, 37.70, 32.21, 31.83, 28.42, 28.33, 27.10, 13.88; DEPT 152.47, 136.51, 135.66, 129.55, 129.21, 126.46, 120.64, 120.07, 119.26, 119.14, 118.22, 113.43, 109.03, 108.91, 108.80, 105.77, 105.28, 55.62, 53.55, 50.14, 49.45, 41.07, 37.69, 29.29, 28.41, 28.34, 27.52, 13.88.

2-((2-((9-ethyl-9H-carbazol-3-yl)amino)-4,4-dimethyl-6-oxocyclohex-1-en-1-yl)(4-(trifluoromethyl)phenyl)methyl)-5,5-dimethylcyclohexane-1,3-dione (Table 2, entry 3, 4c)

Isolated as a brown solid Yield (540 mg 85%); m.p. 98-99°C; FT-IR 3046, 2936, 1594, 1326 cm^{-1}; ^{1}H NMR (400 MHz, CDCl$_3$) δ$_H$; 8.71 (s, 1H, NH), 8.15-8.06 (m, 3H, ArH), 7.87 (s, 1H, ArH), 7.75 (d, J=8.0 Hz, 1H, ArH), 7.59-7.49 (m, 3H, ArH), 7.44 (d, J=12.0 Hz, 2H, ArH), 7.39 (t, J=8.0 Hz, 1H, ArH), 7.29-7.22 (m, 2H, ArH), 5.83 (s, 1H, CH), 4.41 (q, J=7.1 Hz, 2H, CH$_2$), 2.52 (d, J=8.0 Hz, 2H, CH$_2$), 2.47 (s, 2H, CH$_2$), 2.42 (t, J=4.0 Hz, 3H, CH$_2$), 2.36 (s, 1H, CH$_2$), 2.29 (d, J=12.0 Hz, 1H, CH$_2$), 1.46 (t, J=4.0 Hz, 3H, CH$_3$), 1.25 (d, J=8.0 Hz, 5H, CH$_3$), 1.20 (d, J=12.0 Hz, 3H, CH$_3$), 1.12 (s, 2H, CH$_3$), 0.99 (s, 2H, CH$_3$); ^{13}C NMR (125 MHz, CDCl$_3$) δ$_C$; 200.68, 195.69, 177.99, 166.76, 155.70, 142.96, 140.61, 139.24, 128.67, 127.18, 126.09, 125.67, 123.56, 123.08, 122.38, 120.62, 120.03, 119.10, 117.82, 115.16, 114.09, 112.95, 110.89, 108.89, 50.24, 47.05, 46.48, 44.70, 41.07, 37.75, 33.76, 32.30, 31.45, 29.59, 29.33, 27.41, 13.87; DEPT 155.70, 128.67, 127.23, 127.18, 126.45, 126.09, 125.67, 125.63, 125.23, 125.13, 123.83, 120.68, 120.62, 120.03, 119.11, 119.11, 119.26, 117.82, 112.95, 108.89, 50.13, 47.53, 46.49, 44.41, 41.30, 37.66, 33.50, 32.21, 31.43, 29.61, 29.35, 27.73, 13.77; HRMS (ESI/[M + H]$^+$) calcd for C$_{38}$H$_{39}$F$_3$N$_2$O$_3$; 629.2992, found 629.2991.

2-((2-((9-ethyl-9H-carbazol-3-yl)amino)-4,4-dimethyl-6-oxocyclohex-1-en-1-yl)(3-methoxyphenyl)methyl)-5,5-dimethylcyclohexane-1,3-dione (Table 2, entry 4, 4d)

Isolated as a brown solid Yield (415 mg 70%); m.p. 81-82 °C; FT-IR 3052, 2931, 2838, 1589 cm^{-1}; ^{1}H NMR (400 MHz, CDCl$_3$) δ$_H$; 8.65 (s, 1H, NH), 8.11 (d, J=4.0 Hz, 1H, ArH), 8.04 (d, J=1.6 Hz, 1H), 7.60 (s, 1H, ArH), 7.51 (t, J=4.0 Hz, 2H, ArH), 7.44-7.40 (m, 3H, ArH), 7.24 (d, J= 6.2 Hz, 1H, ArH), 7.06-7.03 (dd J$_1$=4.0 Hz, J$_2$=4.0 Hz, 1H, ArH), 6.83 (t, J=8.0 Hz, 1H, ArH), 6.72 (d, J=8.0 Hz, 1H, ArH), 5.30 (s, 1H, CH), 4.42 (q, J= 7.1 Hz, 2H, CH$_2$), 3.93 (s, 3H, OCH$_3$), 2.61 (d, J=4.0 Hz, 1H, CH$_2$), 2.48 (d, J=4.0 Hz, 1H, CH$_2$), 2.43 (d, J=4.0 Hz, 3H, CH$_2$), 2.37 (s, 2H, CH$_2$), 2.34 (s, 1H, CH$_2$), 1.45 (t, J=8.0 Hz, 3H, CH$_3$), 1.24 (s, 3H,

CH$_3$), 1.18 (s, 3H, CH$_3$), 1.15 (s, 3H ,CH$_3$), 0.97 (s, 3H, CH$_3$); ^{13}C NMR (125 MHz, CDCl$_3$) δ$_C$; 200.62, 190.45, 177.87, 166.18, 160.05, 157.94, 143.73, 140.56, 138.87, 138.21, 129.72, 128.91, 128.90, 123.51, 123.11, 122.42, 122.12, 120.60, 120.00, 119.17, 118.92, 112.61, 111.66, 108.79, 55.47, 50.28, 49.77, 47.09, 46.44, 41.02, 37.73, 33.61, 31.39, 29.69, 29.45, 27.35, 13.88; DEPT 154.11, 133.85, 129.65, 126.18, 125.47, 124.84, 122.99, 120.70, 120.63, 120.59, 120.42, 120.08, 119.20, 118.04, 113.17, 108.97, 108.89, 106.35, 53.26, 49.73, 46.79, 44.43, 39.14, 37.37, 33.84, 30.01, 29.41, 28.65, 28.25, 26.19, 13.91; HRMS (ESI/[M + H]$^+$) calcd for C$_{38}$H$_{42}$N$_2$O$_4$; 591.3224, found 591.3223.

2-((2-((9-ethyl-9H-carbazol-3-yl)amino)-4,4-dimethyl-6-oxocyclohex-1-en-1-yl)(4-(methylthio)phenyl)methyl)-5,5-dimethylcyclohexane-1,3-dione (Table 2, entry 5, 4e)

Isolated as a brown solid Yield (524 mg 87%); m.p. 85-86 °C; FT-IR 3041, 2915, 2865, 1594 cm^{-1}; ^{1}H NMR (400 MHz, CDCl$_3$) δ$_H$; 8.60 (s, 1H, NH), 8.10 (d, J=7.7 Hz, 1H, ArH), 8.01 (d, J=1.8 Hz, 1H, ArH), 7.86 (d, J=8.3, 1H, ArH), 7.49-7.47 (m. 1H, ArH), 7.45 (d, J=1.8, 1H, ArH), 7.41 (s, 1H, ArH), 7.39 (s, 1H, ArH) 7.33 (s, 1H, ArH), 7.31 (s, 1H, ArH), 7.21 (d, J=1.0 Hz, 1H, ArH), 7.15 (d, J=8.3 Hz, 1H, ArH), 7.0 (d, J=8.0, 1H, ArH), 5.48 (s, 1H, ArH), 4.37 (q, J=7.2 Hz, 2H, CH$_2$), 2.54 (s, 3H, CH$_3$), 2.51 (d, J=2.9, 1H, CH$_2$), 2.46-2.42 (m, 3H, CH$_2$), 2.35 (t, J=2.7 Hz, 2H, CH$_2$), 2.32 (s, 1H, CH$_2$), 2.28 (s, 1H, CH$_2$), 1.44 (t, J=7.2 Hz, 3H, CH$_2$), 1.36 (t, J=7.2 Hz, 1H, CH$_3$), 1.21 (s, 4H, CH$_3$) 1.13 (s, 2H, CH$_3$), 1.09 (s, 3H, CH$_3$), 0.95 (s, 1H, CH$_3$); ^{13}C NMR (125 MHz, CDCl$_3$) δ$_C$; 190.65, 189.43, 157.25, 143.82, 142.46, 140.57, 138.81, 135.54, 133.47, 128.93, 127.45, 126.81, 125.93, 123.53, 123.13, 120.63, 120.04, 118.94, 115.56, 112.61, 108.84, 108.75, 53.37, 47.10, 46.54, 40.72, 37.71, 32.45, 31.43, 29.69, 29.44, 27.44, 15.20, 13.93; DEPT 157.31, 128.87, 127.36, 126.84, 125.85, 120.58, 120.00, 118.88, 112.48, 108.76, 108.67, 47.07, 46.47, 37.73, 32.40, 29.66, 27.39, 15.24, 13.88; HRMS (ESI/[M + H]$^+$) calcd for C$_{38}$H$_{42}$N$_2$O$_3$S; 607.2995, found 607.2992.

2-((2-((9-ethyl-9H-carbazol-3-yl)amino)-4,4-dimethyl-6-oxocyclohex-1-en-1-yl)(2-nitrophenyl)methyl)-5,5-dimethylcyclohexane-1,3-dione (Table 2, entry 6, 4f)

Isolated as a brown solid Yield (415 mg 68%); m.p. 95-96 °C; FT-IR 3254, 2920, 1517, 1363 cm^{-1}; ^{1}H NMR (400 MHz, CDCl$_3$) δ$_H$; 9.16 (s, 1H, NH), 8.44 (d, J=6.7 Hz, 1H, NH), 8.17-8.14 (m, 2H, ArH), 7.96 (d, J=7.4 Hz, 1H, ArH), 7.77 (t, J=7.7 Hz, 1H, ArH), 7.61-7.57 (m, 2H, ArH), 7.52 (t, J=1.0 Hz, 2H, ArH), 7.47-7.44 (m, 2H, ArH), 7.30 (t, J=4.4 Hz, 1H, ArH), 6.30 (s, 1H, CH), 4.42 (q, J=7.1 Hz, 2H, CH$_2$), 2.60 (s, 1H, CH$_2$), 2.49 (s, 3H, CH$_2$), 2.33 (s, 1H, CH$_2$), 2.19 (s, 2H, CH$_2$), 2.05 (d, J=4.0 Hz, 1H, CH$_2$), 1.45 (t, J=8.0 Hz, 3H, CH$_3$), 1.25 (s, 3H, CH$_3$), 1.17 (s, 3H, CH$_3$), 1.00 (s, 3H, CH$_3$), 0.88 (s, 3H, CH$_3$); ^{13}C NMR (125 MHz, CDCl$_3$) δ$_C$; 200.25, 195.90, 188.17, 152.59, 149.25, 142.67, 140.60, 139.43, 138.63, 134.09, 133.51, 131.60, 130.64, 129.56, 126.51, 126.10, 124.57, 123.06, 120.71, 120.12, 119.16, 118.08, 113.62, 108.91, 50.17, 48.94, 44.76, 40.80, 37.77, 33.06, 31.83, 30.55, 29.96, 28.48, 28.30, 26.32, 13.88; DEPT 188.16, 152.59, 133.50, 131.25, 130.63, 129.56, 126.51, 126.35, 124.56, 124.13, 120.71, 120.12, 119.16, 118.09, 113.61, 108.90, 50.17, 48.95, 44.75, 40.80, 37.77, 30.55, 29.96, 28.48, 28.30, 26.31, 13.88; HRMS (ESI/[M + H]$^+$) calcd for C$_{37}$H$_{39}$N$_3$O$_5$; 606.2969, found 606.2968.

2-((2-((9-ethyl-9H-carbazol-3-yl)amino)-4,4-dimethyl-6-oxocyclohex-1-en-1-yl)(thiophen-2-yl)methyl)-5,5-dimethylcyclohexane-1,3-dione (Table 2, entry 7, 4g)

Isolated as a brown solid, Yield (487 mg 85%); m.p. 113-114 °C; FT-IR 3046, 2926, 1578, 745 cm^{-1}; ^{1}H NMR (400 MHz, CDCl$_3$) δ$_H$; 8.02 (s, 1H, NH), 7.51 (d, J=8.0 Hz, 1H, ArH), 7.44-7.42 (m, 3H, ArH), 7.36 (d, J=8.0 Hz, 2H, ArH), 7.30 (s, 3H, ArH), 6.94-6.91 (dd J$_1$=4.0 Hz, J$_2$=4.0 Hz, 1H, ArH), 5.59 (s, 1H, CH), 4.33 (q, J=7.2 Hz, 2H, CH$_2$), 2.51 (s, J=4.0 Hz, 1H, CH$_2$), 2.43 (d, J=4.0 Hz, 3H, CH$_2$), 2.32 (t, J=8.0 Hz, 3H, CH$_2$), 2.18 (s, 1H, CH$_2$), 1.45 (t, J=8.0 Hz, 3H, CH$_3$), 1.27 (d, J=12.0 Hz, 5H, CH$_3$), 1.17 (d, J=8.0 Hz, 2H, CH$_3$), 1.12 (s, 3H, CH$_3$), 0.99 (s, 1H, CH$_3$), 0.92 (s, 1H, CH$_3$); ^{13}C NMR (125 MHz, CDCl$_3$) δ$_C$; 200.02, 195.60, 178.49, 160.09, 150.72, 143.57, 143.24, 140.59, 138.88, 131.36, 129.49, 127.76, 125.96, 123.51, 123.12, 122.44, 120.70, 120.62, 119.96, 119.24, 118.98, 118.98, 112.81, 108.83, 108.76, 50.13, 49.74, 44.85, 40.91, 37.72, 31.87, 31.22, 29.95, 29.27, 27.09, 13.90;. DEPT 150.76, 131.32, 129.49, 127.72, 125.91, 120.59, 119.95, 118.93, 112.74, 108.77, 108.70, 50.32, 49.67, 44.78, 40.86, 37.95, 31.16, 29.93, 29.27, 28.58, 27.38, 27.01, 13.89; HRMS (ESI/[M + H]$^+$) calcd for C$_{35}$H$_{38}$N$_2$O$_3$S; 567.2682, found 567.2682.

(E)-N-benzylidene-9-ethyl-9H-carbazol-3-amine (Table 2, entry 1, 5a)

Isolated as a brown solid Yield (36 mg 12%); m.p.82-83 °C; FT-IR 1610 cm^{-1}; ^{1}H NMR (400 MHz, CDCl$_3$) δ$_H$; 8.71 (s, 1H, C=N), 8.23 (d, J=8.0 Hz, 1H, ArH), 8.15 (d, J=4.0 Hz, 1H, ArH), 8.07-8.05 (m, 2H, ArH), 7.57-7.53 (m, 1H, ArH), 7.42 (t, J=8.0 Hz, 4H, ArH), 7.35 (m, 2H, ArH), 4.35 (q, J=7.1 2H, CH$_2$), 1.45 (t, J=8 Hz, 3H, CH$_3$); ^{13}C NMR (125 MHz, CDCl$_3$) δ$_C$; 158.02, 143.82, 140.59, 136.81, 130.93, 128.83, 128.65, 125.98, 123.54, 123.15, 120.66, 120.05, 118.98, 112.69, 108.87, 108.78, 37.70, 13.92.

(E)-N-((2-chloro-6-methoxyquinolin-3-yl)methylene)-9-ethyl-9H-carbazol-3-amine (Table 2, entry 2, 5b)

Isolated as a brown solid Yield (42 mg 10%); m.p. 182-183 °C; FT-IR 1616, 597 cm^{-1}; ^{1}H NMR (400 MHz, CDCl$_3$) δ$_H$; 9.11 (s, 1H, C=N), 8.92 (d, J=8.0 Hz, 1H, ArH), 8.15-8.11 (m, 2H, ArH), 7.92 (d, J=8.0 Hz, 1H, ArH), 7.57 (d, d J$_1$=1.6 Hz, J$_2$=1.6, 1Hz, ArH), 7.48 (t, J=8.0 Hz, 1H, ArH), 7.41 (t, J=8.0 Hz, 1H, ArH), 4.37 (q, J=7.1 Hz, 2H, CH$_2$), 3.92 (s, 3H, OCH$_3$) 1.44 (t, J=8.0 Hz, 3H, CH$_3$); ^{13}C NMR (125 MHz, CDCl$_3$) δ$_C$; 158.37, 152.62, 147.81, 144.39, 142.97, 140.58, 139.34, 135.69, 129.67, 128.38, 128.09, 126.50, 126.11, 124.41, 123.57, 123.05, 120.66, 120.05, 119.15, 113.44, 108.90, 108.78, 105.81, 55.63, 37.72, 13.87; HRMS (ESI/[M + H]$^+$) calcd for C$_{25}$H$_{20}$ClN$_3$O; 414.1374, found 414.1373.

(E)-9-ethyl-N-(4-(trifluoromethyl)benzylidene)-9H-carbazol-3-amine (Table 2, entry 3, 5c)

Isolated as a brown solid Yield (23 mg 7%); m.p. 108-109°C; FT-IR 1621, 1326 cm^{-1}; ^{1}H NMR (400 MHz, CDCl$_3$) δ$_H$; 8.71(s, 1H, C=N), 8.15-8.06 (m, 4H, ArH), 7.75 (d, J=8.0 Hz, 2H, ArH), 7.54-7.49 (m, 2H, ArH), 7.43 (d, J=8.0 Hz 2H, ArH), 7.27 (s, 1H, ArH), 4.41 (q, J=7.3 Hz, 2H, CH$_2$), 1.45 (t, J=8.0 Hz, 3H, CH$_3$); ^{13}C NMR (125 MHz, CDCl$_3$) δ$_C$; 155.73, 142.98, 140.60, 139.23, 128.65, 126.07, 125.71, 123.07, 120.61, 120.01, 119.09, 112.90, 108.86, 108.78, 37.76, 13.87; HRMS (ESI/[M+H]$^+$) calcd. for C$_{22}$H$_{17}$F$_3$N$_2$; 367.1423, found 367.1422.

(E)-9-ethyl-N-(3-methoxybenzylidene)-9H-carbazol-3-amine (Table 2, entry 4, 5d)

Isolated as a brown solid Yield (48 mg 14%); m.p. 78-79 °C; FT-IR 1589, 2915 cm^{-1}; ^{1}H NMR (400 MHz, CDCl$_3$) δ$_H$; 8.60 (s, 1H, C=N), 8.12 (d, J=8.0 Hz, 1H, ArH), 8.01 (s, 1H, ArH), 7.92 (d, J=8.0 Hz, 2H, ArH), 7.48-7.40 (m, 4H, ArH), 7.23 (d, J=8.0 Hz, 1H, ArH), 7.00 (d, J=12.0 Hz, 2H, ArH), 4.41 (q, J=7.2 Hz, 2H, CH$_2$), 1.45 (t, J=8.0 Hz, 3H, CH$_3$); ^{13}C NMR (125 MHz, CDCl$_3$) δC 161.89, 157.63, 144.22, 140.52, 138.59, 130.22, 129.80, 125.81, 123.49, 123.11, 120.57, 119.99, 118.80, 114.18, 112.31, 108.72, 108.63, 55.43, 37.70, 13.88.

(E)-9-ethyl-N-(4-(methylthio)benzylidene)-9H-carbazol-3-amine (Table 2, entry 5, 5e)

Isolated as a brown solid Yield (33 mg 9%); m.p. 138-139 °C; FT-IR 1589, 2871 cm^{-1}; ^{1}H NMR (400 MHz, CDCl$_3$) δ$_H$; 8.61 (s, 1H, C=N), 8.12 (d, J=8.0 Hz, 1H, ArH), 8.02 (s, 1H, ArH), 7.88 (d, J=8.0 Hz, 2H, ArH), 7.48 (t, J=8.0 Hz, 2H, ArH), 7.42-7.40 (m, 2H, ArH), 7.34 (d, J=8.0 Hz, 2H, ArH), 7.25 (d, J=8.0 Hz, 1H, ArH), 4.38 (q, J=4.6 Hz, 2H, CH$_2$), 2.55 (s, 3H, SCH$_3$), 1.45 (t, J=8.0 Hz, 3H, CH$_3$); ^{13}C NMR (125 MHz, CDCl$_3$) δ$_C$; 157.28, 143.87, 142.40, 138.78, 133.50, 128.88, 125.86, 123.52, 123.11, 120.58, 119.99, 118.88, 112.50, 108.76, 108.67, 37.72, 15.23,

13.87; HRMS (ESI/[M + H]$^+$) calcd for C$_{22}$H$_{20}$N$_2$S; 345.1426, found 345.1425.

(*E*)-9-ethyl-*N*-(2-nitrobenzylidene)-9*H*-carbazol-3-amine (Table 2, entry 6, 5f)

Isolated as a brown solid Yield (77 mg, 22%); m.p. 140-141 °C; FT-IR 1610, 1331 cm^{-1}; ^{1}H NMR (400 MHz, CDCl$_3$) δ$_H$; 9.15 (s, 1H, C=N), 8.43 (d, J=8.0 Hz, 1H, ArH), 8.15 (t, J=8.0 Hz, 2H, ArH), 8.08 (d, J=8.0 Hz, 1H, ArH), 7.75-7.55 (m, 1H, ArH), 7.50 (d, J=8.0 Hz, 2H, ArH), 7.49-7.42 (m, 1H, ArH), 7.28 (d, J=8.0 Hz, 2H, ArH), 7.25 (d, J=8.0 Hz, 1H, ArH), 4.39 (q, J=4.0 Hz, 2H, CH$_2$), 1.48 (t, J=8.0 Hz, 3H, CH$_3$) ^{13}C NMR (125 MHz, CDCl$_3$) δ$_C$: 152.57, 149.28, 142.70, 140.61, 139.44, 133.48, 130.61, 129.57, 126.10, 124.56, 123.56, 123.07, 120.71, 120.11, 119.16, 113.62, 108.89, 108.77, 37.77, 13.87.

(*E*)-9-ethyl-*N*-(thiophen-2-ylmethylene)-9*H*-carbazol-3-amine (Table 2, entry 8, 5g)

Isolated as a brown solid, Yield (33 mg, 10%); m.p. 210-211 °C; FT-IR 1605, 717 cm^{-1}; ^{1}H NMR (400 MHz, CDCl$_3$) δ$_H$; 8.78 (s, 1H, C=N), 8.12 (d, J=8.0 Hz, 1H, ArH), 8.00 (d, J=1.4 Hz, 1H, ArH), 7.50-7.47 (m, 3H, ArH), 7.43-7.39 (m, 1H, ArH), 7.22 (d, J=8.0 Hz, 2H, ArH), 7.15 (t, J=4.0 Hz, 1H, ArH), 4.37 (q, J=7.2 Hz, 2H, CH$_2$), 1.45 (t, J=8.0 Hz, 3H, CH$_3$); ^{13}C NMR (125 MHz, CDCl$_3$) δ$_C$; 150.76, 143.52, 143.23, 140.54, 138.84, 131.30, 129.49, 127.71, 125.91, 123.47, 123.09, 120.60, 119.95, 118.92, 112.73, 108.75, 108.69, 37.72, 13.89; HRMS (ESI/[M+H]$^+$) calcd for C$_{19}$H$_{16}$N$_2$S; 305.1113, found 305.1111.

G.Thirunarayanan, Department of chemistry, Annamalai University, Annamalainagar-608 002, Tamilnadu, India.
Tel.: +91 4144 220015.E-mail: drgtnarayanan@rediffmail.com

† Electronic Supplementary Information (ESI) available: [UV-Viss DRS spectra of SnO$_2$-fly ash and SO$_4^{2-}$SnO$_2$-fly ash. EDS spectra of catalyst atomic and weight precentage Table S1. The synthsized compounds of 4a-4g and 5a-5g spectra of NMR and HRMS (4a, 4c, 4d, 4e, 4f, 4g and 5b, 5c, 5e, 5f and 5g).]. See DOI: 10.1039/b000000x/

Notes and references

1   C. -J. Li, T. H. Chan, Comprehensive Organic Reactions in Aqueous Media, 2nd ed. Wiley: New York, 2007.
2   (a) C. -J. Li, *Chem. Rev.,* 2005, **105**, 3095-3165. (b) R. N. Butler and A. G. Coyne, *Chem. Rev*., 2010, **110**, 6302-6337. (c) M.-O. Simon and C. -*J*. Li,. *Chem. Soc. Rev.,* 2012, **41**,1415-1427.
3   J. Grunes, J.Zhu. and G. A. Somorjai, *Chem. Commun.,* 2003, **18**, 2257-2260.
4   D. Astruc, F. Lu and J. R. Aranzaes, *Angew. Chem., Int. Ed.,* 2005, **44**, 7852-7872.
5   (a) K. Shimizu, R. Sato and A. Satsuma, *Angew. Chem., Int. Ed.,* 2009, **48**, 3982-3986. (b) C. A. Witham, W. Huang, C. Tsung, J. N. Kuhn, G. A. Samorjai and F. D. Toste, *Nat. Chem.,* 2009, **2**, 36-41.
6   G. Thirunarayanan, P. Mayavel and K. Thirumurthy, *Spectr. Acta. A.,* 2012, **91**, 18-22.
7   C. P. Nicholas and T. J. Marks, *Nano Lett.*, 2004, **4**, 1557-1559.
8   H. Matsuhashi, H. Miyazaki, Y. Kawamura, H. Nakamura and K. Arata, *Chem. Mater.*, 2001, **13**, 3038-3042.
9   M. K. Lam, K. T. Lee and A. R. Mohamed, *Appl. Catal. B.*, 2009, **93**, 134-139.
10 H. Matsuhashi, T. Tanaka and K. Arata, *J. Phy. Chem. B.,* 2001, **105**, 9669-9671.
11 V.Ponec and G. C. Bond, *Stud. Surf. Sci. Catal.,* 1995, **95**, 477-539.
12 S. R. Sarda, V. A. Puri, A. B. Rode, T. N. Dalawe, W. N. Jadhav and R. P. Pawar, *Arkivoc.*, 2007, **2**, 246-251.
13 M. A. Naik, B. G. Mishra, A. Dubey and G. D. Hota., *Bull. Catal Soci., India.*, 2009, **8**, 35-40.
14 M. Sowmiya, A. Sharma, A. Parsodkar, B. G. Mishra and A. Dubey, *Appl. Catal. A.,* 2007, **333**, 272-280.
15 S. P. Chavan, P. K. Zubaidha, S. W. Dantale, A. Kesavaraja, A. V. Ramaswamy and T. Ravindranathan, *Tetrahedron.,* 1996, **37**, 233-236.
16 Y. Du, S. S. Liu, Y. Zhang, C. Yin, Y. Di and F. -S. Xiao, *Catal. Lett.*, 2006, **108**, 155-158.
17 S. Furuta, H. Matsuhashi and K. Arata, *Appl. Catal. A.*, 2004, **269**, 187-191.
18 J. I. Moreno, R. James, R. Gómez and M. E. Niño- Gómez, *Catal. Today.*, 2011, **172**, 34-40.
19 S. A. Dake, M. B. Khedkar, G. S. Irmale, S. J. Ukalgaonkar, V. V. Thorat, S. A. Shintre and R. P. Pawar, *Synth. Commun.,* 2012, **42**, 509-1520.
20 T. R. Gaydhankar, P. N. Joshi, P. Kalita and R. Kumar, *J. Mole. catal. A:Chem.,* 2006, **265**, 306-315.
21 N. R. Monks, D. C. Blankey, S. J. East, R. I. Dowell, J. A. Caluete, N. J. Curtin, C. E. Arris and D. R. Newell, *Eur. J. Cancer.,* 2002, **38**, 1543-1552.
22 J. C. Wang, *Biochem.,* 1996, **65**, 635-692.
23 J. H. Burroughes, D. D. C. Bradley, A. R. Brown, R. Marks, N. K. Mackay, R. H. Friend and A. B. Holmes, *Nature.*, 1990, **347**, 539-541.
24 R. H. Friend, R. W. Gymer, A. B. Holmes, J. H. Burroughes, R. N. Marks, C. Taliani, D. D. C. Bradley, D. A. Santos, J. L. Bredas, M. Logdlund and W. R. Salaneck, *Nature.,* 1999, **397**, 121-128.
25 (a) G. Horowitz, R. Hajlaoui, D. Fichou and A. E. Kassmi, *J. Appl. Phys.,* 1999, **85**, 3202-3206. (b) Y. Zhang, T. Wada and H. Sasabe, *J. Mater. Chem.*, 1998, **8**, 809-828.
26 J. -F Morin, M. Leclerc, D. Ades and A. Siove, *Macromol. Rapid Commun.*, 2005, **26**, 761-778.
27 S. M. Vahdat and S. Baghery, *Het. Let. Org.*, 2012, **2**, 43-51.
28 S. M. Vahdat and M. Akbari, *Orie. J. Chem.*, 2011, **27**, 1573-1580.
29 J. S. Ghomi, M. A. Ghasemzadeh, and S. Zahedi, *J. Mex. Chem. Soc.*, 2013, **57**, 1-7.
30 H. Zang, Y. Zhang, Y. Zang and B. W. Cheng, *Ultrason. Sonochem.,* 2010, **17**, 495-499.
31 V. A. Chebanov, V. E. Saraev, S. M. Desenko, V. N. Chernenko, I. V. Knyazeva, U. Groth, T. N. Glasnov, and C. O. Kappe, *J. Org. Chem.,* 2008, **73**, 5110-5118.
32 Y. -J. Zhou, D. -S. Chen, Y. -L. Li, Y. Liu, and X. -S. Wang, *ACS Comb. Sci.*, 2013, **15**, 498-502.
33 R. G. -Vagheia, and S. M. Malaekehpoor, *J. Iran. Chem. Soc.,* 2010, **7**, 957-964.
34 S. Sudha and M. A. Pasha, *The Sci world J.* 2013, Article ID 930787.
35 W. K. Anderson, E. J. L.Voie, and P. G. Whitkop, *J. Org. Chem.,* 1974, **39**, 881-884.
36 T. Toupance, O. Babot, B. Jousseaume and G. Vilaca, *Chem. Mater.,* 2003, **15**, 4691-4697.
37 Z. L. Butsko and P. M. Standik, Influence of an electrical field on the structure of a silica gel. D. N. Strazhesko (Eds), Adsorption and adsorbents, New York: John Willey & Sons; 1, 1973. 96-100.
38 B. J Saikia, G. Parthasarthy, N. C. Sarmah and G. D. Barvah, *Bull. Mater. Sci.*, 2008, **31**, 155-158.
39 S. Loridant, *J. Phys. Chem. B.,* 2002, **106**, 13273-13279.
40 G. Xi and J. Ye, *Inorg.Chem.,* 2010, **49**, 2302-2309.
41 L. Abello, B. Bocha, A. Gaskov, S. Koudryavtseva, G. Lucazesu and M. Romyantseva, *J. Solid. State chem.,* 1998, **135**, 78-85.
42 B. Cheng, J. M. Russell, W. Shi, L. Zhang and E. T. Samulski, *J.Am. Chem. Soc.,* 2004, **126**, 5972-5973.
43 D. Jain, M. Mishra and A. Rani, *Fuel. Proc. Tech.*, 2012, **95**, 119-126.

44 I. G. Lodeiro, A. Palomo, and A. F. -Jimenez, *Ceme & Concre Res.*, 2007, **37**, 175-183.

45 J. Haines, *France private commun.*,1998.

46 A. Caron and F. Donohue, *Acta Crystal.*, 1965, **18**, 562-565.

5 47 H. Wang, Q. Liang, W. Wang, Y. An, J. Li, and L. Guo, *Cryst. Growth Des.,* 2011, **11**, 2942–2947.

48 A. Corma and H. Garcıa, *Chem. Rev.,* 2002, *102,* 3837-3892.

49 J. -M. Jehng, *J. Phys. Chem. B.,* 1998, **102**, 5816-5822.

50 S. Nishiyama, T. Hara, S. Tsuruya and M. Masai, *J. Phys. Chem. B.,* 10 1999, **103**, 4431-4439.

51 A. Corma, L. T. Nemeth, M. Renz, and S. Valencia, *Nature.*, 2001, **412**, 423-425.

52 I. R. Beattie, *Quart. Rev. (London).*, 1963, **17**, 382-389.

53 (a) M. S. Holt, W. L. Wilson, and J. H. Nelson, *Chem. Rev.*, 1989, 15 **89**, 11-49. (b) S. Hermans and B. F. G. Johnson, *Chem. Commun.*, 2000, **19**, 1955-1956.

54 G. W. Huber, J. W. Shabaker and J. A. Dumesic, *Science.*, 2003, **300**, 2075-2077.

20